# Energy Optimization through Cooperative Storage Management: A Calculus of Variations Approach

Johann Leithon*

*Department of Signal Processing and Acoustics, Aalto University, e-mail: johann.leithon@aalto.fi*

Stefan Werner

*Department of Electronic Systems, Norwegian University of Science and Technology, e-mail: stefan.werner@ntnu.no.*

Visa Koivunen

*Department of Signal Processing and Acoustics, Aalto University, e-mail: visa.koivunen@aalto.fi*

**Abstract**

A framework to optimize energy utilization through battery management in a cooperative environment is proposed. Participating households share access to a community-owned energy farm and are equipped with lossy rechargeable batteries. The proposed optimization framework aims to minimize energy expenditure while accounting for time- and location-dependent electricity prices. The battery discharging schedules are optimized by using elements of calculus of variations and optimal control theory. The energy allocation policy is designed by solving an optimization problem through Lagrange Multipliers. Continuous-time optimization techniques are used to provide explicit solutions to the mathematical problems and determine closed-form performance estimates. The derived analytical expressions can be used to reduce the computational complexity of existing strategies, size energy storage systems, estimate performance bounds, and gain relevant insights. Extensive simulations are presented to validate the theoretical analysis and evaluate the impact of different system parameters. Specifically, cost savings are assessed as a function of discharging efficiency rates and nominal output power. It is shown that higher efficiency rates in battery operations lead to a an increased price-selectivity of the proposed algorithm.

*Keywords:* Energy optimization, storage management, calculus of variations, Karush-Kuhn-Tucker conditions, Peukert's Law.

## 1. Introduction

In countries from the Organization for Economic Co-operation and Development (OECD), the production of solar (photovoltaic) energy has increased from 19 GWh in 1990 to 106.4 TWh in 2013,

*The work of Dr. Werner was supported, in part, by the Research Council of Norway.
*Corresponding author

International Energy Agency (2014). This trend has favored the adoption of distributed generators, making the energy production and the grid itself less centric, Dimitrov et al. (2016). Many consumers have opted for deploying their own solar panels, while others have chosen to team up and share energy generation and storage infrastructure, Feldman et al. (2015).

Among other benefits, distributed generation can contribute to a reduced peak-to-average power ratio, Zhao et al. (2017), and thereby a more resilient grid, Sandgani and Sirouspour (2017), Gatsis and Giannakis (2013). However, solar generation is characterized by intermittency, which often results in increased operational costs for utilities and consumers, Zhang et al. (2014). To cope with such uncertainty, energy storage systems (ESSs) can be introduced, thus allowing users to schedule their grid energy consumption, Rahbar et al. (2016), Wang et al. (2013), Rastegar et al. (2017), take advantage of time-varying pricing and energy production, Ratnam et al. (2015), Pilloni et al. (2018), Ranaweera and Midtgård (2016), and reduce their electricity costs by participating in demand response programs, Wang et al. (2013), Hooshmand and Rabiee (2019), Tushar et al. (2016), Nunna et al. (2016), Cortés-Arcos et al. (2017). Distributed ESSs can also be used in load balancing applications, Bayram et al. (2017), Paridari et al. (2015), combat over-voltage issues, Ranaweera et al. (2017), and to enable self-sustainable micro and nanogrids, Liu et al. (2018).

To improve the capacity of the ESSs, and reduce the effects of untimely solar generation, proper energy management algorithms can be devised. Moreover, given the increasing popularity of cooperation schemes such as shared solar, Feldman et al. (2015), these energy management algorithms will also need to account for multiple participants in collaborative environments. In that context, this paper proposes ESS-enabled energy cooperation strategies for households with shared access to a community-owned energy farm.

The proposed energy cooperation strategy aims at minimizing the energy expenditure incurred by participating households over a finite planning horizon. Each household is equipped with a lossy rechargeable battery, which is characterized by a limited storage capacity and a non-linear discharging behavior. Unlike existing works, the battery model used in this study takes into account the non-linear relationship between the discharging rate and the charge remaining in the battery. Energy management strategies that are aware of such non-linear behavior can lead to extended battery lifetimes, Tran and Khambadkone (2013), and higher cost savings, Leithon et al. (2016).

To devise the proposed strategy, the optimization problem is divided into two subproblems. The first subproblem concerns the battery discharging operation. That is, subject to relevant causality constraints, the battery discharging operation is optimized within each household. A second optimization problem is formulated to allocate the energy of the farm across participating households, while enforcing constraints derived from the law of conservation of energy. Closed-form analytical solutions are provided for relaxed versions of the two optimization problems. These estimates can be used to

assess the impact of different system parameters in the achieved savings.

### 1.1. Related Works

Storage sharing for energy management has been explored extensively in recent years. For example, cost-minimization strategies leveraging shared ESSs have been proposed by Sandgani and Sirouspour (2017), Rahbar et al. (2016), Dimitrov et al. (2016), Wang et al. (2013), Paridari et al. (2015), AlSkaif et al. (2015) and Leithon et al. (2018), among others. Some of these works have considered renewable energy assets as well, e.g., Sandgani and Sirouspour (2017) and Rahbar et al. (2016).

More general storage sharing strategies for utility maximization have been proposed by Wang et al. (2018) and Tushar et al. (2016). Similarly, strategies based on shared ESSs have been designed for peak load shaving applications by Bayram et al. (2017) and Zhao et al. (2017). An energy trading system for users with shared access to an ESS has been proposed by Mediwaththe et al. (2016). In most of these works, the shared asset is the storage capacity of the ESSs, not their stored energy. Moreover, the ESSs have been modeled as linear devices in most cases.

Cooperative energy management strategies have been proposed by Ye et al. (2017), Etesami et al. (2018), Zhang et al. (2013), Stoyanova et al. (2014), Luna et al. (2016), Mangiatordi et al. (2016), Rahbar et al. (2016), Dagdougui et al. (2016), AlSkaif et al. (2015), Xu et al. (2017), Hammad et al. (2015), Zhou et al. (2018), and Marzband et al. (2018). The strategy presented by Ye et al. (2017) leverages energy sharing and time-varying electricity prices to minimize the energy expense incurred by the participating households over a finite planning horizon. Zhang et al. (2013) proposes a technique to solve the economic dispatch problem in a decentralized manner by using agent cooperation across locations. Similarly, Stoyanova et al. (2014) and Mangiatordi et al. (2016) devised strategies to reduce grid losses through load scheduling, or power flow optimization. Luna et al. (2016) developed a strategy to reduce the disconnection of the load by coordinating the operation of distributed household prosumers. The strategies proposed by Zhang et al. (2013), Rahbar et al. (2016), Dagdougui et al. (2016), and Hammad et al. (2015) optimize energy utilization in microgrids and buildings through energy sharing and storage management.

Coalitional game theory based methods optimizing the use of energy storages and renewable energy sources within a community of residential households were proposed by Chiş and Koivunen (2019). The cost savings achieved by the coalitional optimization are divided among the participating households in a fair manner.

Unlike the works listed above, this paper studies the energy optimization problem by accounting for both location- and time-dependent electricity prices, as well as distributed ESSs. Moreover, the ESS model used in this paper considers the non-linear characteristics of the discharging operation, which allows for higher performance and a longer battery lifespan, Tran and Khambadkone (2013).

This paper extends previous work on cooperative energy management assuming linear ESSs, Leithon et al. (2020).

### *1.2. Contributions and Organization of the Paper*

The contributions of this paper are the following: First, an optimization framework is proposed to devise energy cost minimization strategies for users with shared access to an energy farm. The proposed optimization framework accounts for non-linear discharging losses and electricity prices that vary across time and location. Second, closed-form expressions are derived to estimate the optimal energy consumption profile across time and the achievable cost savings attained both individually and collectively. The proposed strategies do not require load scheduling, and as such, they can be applied to households with limited flexibility to schedule their power consumption.

This paper is organized as follows: Sec. 2 describes the system model and lays out the mathematical framework. Sec. 3 presents the formulation of the mathematical problem to determine both the optimal battery discharging profiles and the optimal policy for energy allocation across users. This section also discusses a computationally-intensive numerical approach that can be used to find an approximate solution to the optimization problem. In Sec. 4, the proposed solution is presented in two parts: First, the battery discharging operation is optimized by using calculus of variations, Giaquinta et al. (2004). Second, the optimal energy allocated to each household is computed by using the method of Lagrange multipliers (Karush-Kuhn-Tucker conditions), see Boyd and Vandenberghe (2004). In Sec. 5, numerical results are used to validate the analytical results developed in the paper. Finally, conclusions are presented in Sec. 6.

## 2. System Model

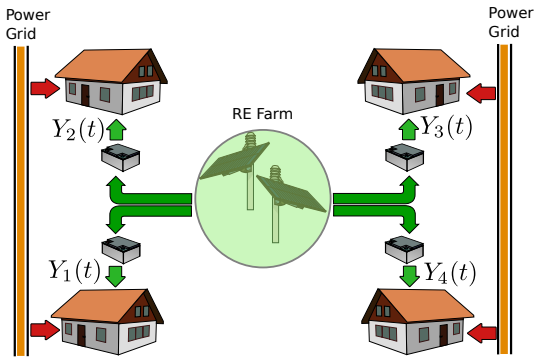


Figure 1: System setup: Battery-equipped households with shared access to an energy farm.

### 2.1. System Setup

This study considers a community of $M \in \mathbb{N}$ grid-connected cooperating households with shared access to an energy farm. Fig. 1 illustrates the system setup with $M = 4$. The energy available in the energy farm is allocated to the households on a day-ahead basis and in order to minimize their collective energy expenditure.

### 2.2. Loads, Pricing Model, and Planning Horizon

To ensure generality, the power demand at each household is considered non-deferrable,[1] and denoted by $L_i(t)$, where $t$ is the time index, continuous from 0 to $T \in \mathbb{R}_+$. The planning horizon is thus $[0, T]$ and can be arbitrarily large.

The electricity prices offered to household $i$ are denoted by $P_i(t) > 0,\ \forall\ t$. The power consumed by the $i$th household from the storage is denoted by $Y_i(t)$, and the energy cost incurred by the $i$th household in $[0, T]$ is

$$\int_0^T P_i(t)\left[L_i(t) - Y_i(t)\right] dt.$$

Then, the total energy cost incurred by the set of cooperating households in $[0, T]$ is

$$\mathsf{EC} = \sum_{i=1}^{M} \int_0^T P_i(t)\left[L_i(t) - Y_i(t)\right] dt, \tag{1}$$

where $Y_i(t) \leq L_i(t),\ \forall\ t,\ \forall\ i$. This cost function allows for discrete-time pricing schemes too, as $P_i(t)$ can be defined as a linear combination of step functions.

### 2.3. Energy Storage Systems (ESSs)

The following characteristics of the ESSs in the system are assumed (to maintain generality, characteristics such as size and efficiency rate can vary across households):

- Dynamics of the ESSs: The energy available in the ESS at the $i$th household is denoted by $E_i(t)$, and evolves according to:

$$E_i(t) = E_i(0) - \int_0^t X_i(\tau) d\tau, \tag{2}$$

where $E_i(0)$ is the energy allocated at the beginning of the planning period, $X_i(t)$ is the power drawn by the $i$th household before losses. It follows that $X_i(t) \geq Y_i(t),\ \forall\ t,\ \forall\ i$, since the ESS incurs power loss in the discharging operation. Moreover, losses incurred in the charging operation are accounted for implicitly.

[1] If the households' power consumption can be scheduled, further cost reduction can be achieved using existing load scheduling algorithms.

- Non-linear discharging losses: Each ESS in the system is subject to discharging losses, which are modeled using Peukert's law, Linden and Reddy (2001). Peukert's law can be used to estimate the relationship between the power drawn from a rechargeable battery and its remaining capacity. This modeling approach is useful because of its simplicity and acceptable accuracy in lead-acid batteries. By using Peukert's law, the relationship between $X_i(t)$ and $Y_i(t)$ can be estimated as follows:

$$Y_i(t) = \min\left\{X_i(t), \Psi_i\left[\frac{X_i(t)}{\Psi_i}\right]^{\frac{1}{\alpha_i}}\right\}, \tag{3}$$

where $\Psi_i > 0$ and $\alpha_i > 1$ are, respectively, the rated output power, and Peukert's exponent (battery efficiency parameter). As seen in (3), $X_i(t) \geq Y_i(t),\ \forall\, i\, \forall\, t$, which models the occurrence of power loss in the discharging operation, particularly when $X_i(t) > \Psi_i$. For ease of notation, the relationship between $Y_i(t)$ and $X_i(t)$ can be described by using the function $f_i : \mathbb{R} \to \mathbb{R}$. That is, for any $t \in\ [0, T]$, it follows that $Y_i(t) = f_i\left(X_i(t)\right)$, where

$$f_i(x) \triangleq \min\left\{x, \Psi_i\left[\frac{x}{\Psi_i}\right]^{\frac{1}{\alpha_i}}\right\}.$$

- Limited storage capacity: The capacity of the ESS at the $i$th household is denoted by $\Theta_i$. Therefore, the energy stored in the $i$th battery satisfies

$$0 \leq E_i(t) \leq \Theta_i, \forall\ t\ \in\ [0, T]. \tag{4}$$

To ensure full battery depletion at the end of the planning period, the following set of constraints will be imposed on each $Y_i(t)$:

$$E_i(T) = 0,\ \forall\ i\ \in\ \{1, \ldots, M\}. \tag{5}$$

### *2.4. Connectivity and Information Requirements*

The strategy developed in this paper is centralized, and as such, it uses information shared among participating households. The participating households and the RE farm will need to exchange information by using a communication system comprised of a control center, a gateway, and smart meters deployed in each household. A description of each of these components is provided by Bao and Lu (2015). The smart meters are equipped with communication and power-switching mechanisms, Sun et al. (2016). Hence, power source switching and battery discharging circuitry can be centrally controlled following the optimization strategy proposed in Sec. 4.

## 3. Problem Formulation and Numerical Solution

### *3.1. Problem Formulation*

Let $E_0 > 0$ denote the total energy initially available for allocation across households; then, without loss of generality, the battery discharging profiles and the energy allocation policy, can both be designed

in terms of $E_0$. To jointly design the battery discharging profiles and the energy allocation policy, the following optimization problem is formulated:

$$\text{P0:} \min_{E_i(0), Y_i(t),\ i\in\ \{1,\ldots,M\}} \sum_{i=1}^{M} \int_0^T P_i(t)\left[L_i(t) - Y_i(t)\right] dt$$

s.t.

$$0 \le E_i(t) \le \Theta_i, \forall\ i,\ t,$$

$$E_i(T) = 0,\ \forall\ i$$

$$0 \le Y_i(t) \le L_i(t), \forall\ i,\ t$$

$$E_i(0) \ge 0,\ \forall\ i,\ \text{and}$$

$$\sum_{i=1}^{M} E_i(0) = E_0,$$

with:

$$Y_i(t) = \min\left\{X_i(t), \Psi_i\left[\frac{X_i(t)}{\Psi_i}\right]^{\frac{1}{\alpha_i}}\right\},$$

and

$$E_i(t) = E_i(0) - \int_0^t X_i(\tau) d\tau.$$

As seen in P0, the decision variables are non-negative numbers $E_1(0), \ldots, E_M(0)$ and trajectories $Y_1(t), \ldots, Y_M(t)$. Note that the problem can also be formulated in terms of $X_1(t), \ldots, X_M(t)$, given the one-to-one relationship between $Y_i(t)$ and $X_i(t)$ in (3). In fact, a more stringent version of constraint $0 \le Y_i(t) \le L_i(t), \forall\ i,\ t$ can be stated in terms of $X_i(t)$ as $0 \le X_i(t) \le L_i(t), \forall\ i,\ t$. Clearly, imposing constraint $0 \le X_i(t) \le L_i(t), \forall\ i,\ t$ will shrink the feasible space, given that, by virtue of the discharging losses, the trajectories $Y_i(t)$ and $X_i(t)$ satisfy $Y_i(t) \le X_i(t),\ \forall\ t,\ i$. Such tightening of constraints will be used to find feasibility conditions for P0 in terms of both the $L_i(t)$'s and $E_0$.

### *3.2. Properties of the Optimization Problem and Feasibility*

Although the problem can be stated in a simple notation, it admits interesting challenges. P0 is not a convex optimization problem because its objective is a functional, i.e., a function of functions, and the inequality (4) states an infinite (and uncountable) number of constraints. Solving P0 means finding the optimal battery discharging profiles and the energy allocation strategy that minimizes the collective energy cost over the entire planning period $[0, T]$.

P0 is infeasible if the $L_i(t)$'s are such that the total RE, $E_0$, cannot be fully utilized in $[0, T]$. Moreover, constraint $E_i(T) = 0,\ \forall\ i$ implies

$$\sum_{i=1}^{M} \int_0^T X_i(\tau) d\tau = \sum_{i=1}^{M} E_i(0) = E_0, \tag{6}$$

since $E_i(0) = \int_0^T X_i(\tau)d\tau$. Following (6), the total amount of energy utilized in $[0, T]$ by the $M$ participants is $E_0$, the energy initially available for allocation.

In the following, a necessary condition for the feasibility of P0 is established in terms of $L_1(t), \ldots, L_M(t)$ and $E_0$. First, constraint $Y_i(t) \leq L_i(t)$ is relaxed to $\int_0^T Y_i(t)dt \leq \int_0^T L_i(t)dt$. Then, by using $\int_0^T Y_i(t)dt \leq \int_0^T X_i(t)dt, \ \forall \ i, \ t$ the following condition can be written:

$$0 \leq 2\int_0^T Y_i(t)dt \leq \int_0^T L_i(t)dt - \int_0^T X_i(t)dt,$$

which, given (6), implies:

$$\sum_{i=1}^{M} \int_0^T L_i(\tau)d\tau \geq E_0. \tag{7}$$

Eq. (7) states a necessary condition for P0 to be feasible. This condition simply states that the RE allocated at the beginning of the planning period must be at most equal to the expected load across all participating households.

### *3.3. Numerical Solution*

This section discusses how to solve P0 numerically. First, discretization in time is introduced. Then, a linearization of $f_i(x)$ is used to simplify the relationship between $X_i(t)$ and $Y_i(t)$. This approach can be used to find approximate solutions in response to available computational resources. Specifically, the sampling rates and the quality of the linearization can be adjusted to match available resources while producing solutions with different levels of accuracy. A more analytical approach is proposed in Sec. 4, where optimization techniques are combined to obtain an approximate solution in closed form.

#### *3.3.1. Discretization in Time*

Let $\Delta t > 0$ denote the sampling interval, and consider $N > 0$ samples in $[0, T]$. Then, by replacing definite integrals with sums, the objective function in P0 can be written in the discrete domain as follows:

$$\widetilde{\mathsf{EC}} = \sum_{i=1}^{M} \Delta t \sum_{k=1}^{N} P_i(k\Delta t) \left[ L_i(k\Delta t) - Y_i(k\Delta t) \right]. \tag{8}$$

Then, a discrete representation of P0 can be cast as follows

$$\text{P0D:} \min_{E_i(0), Y_i(k\Delta t),\ i\in\{1,\dots,M\},\ k\in\{1,\dots,N\}} \widetilde{\mathsf{EC}}$$

s.t.

$$0 \le E_i(k\Delta t) \le \Theta_i, \forall\ i,k,$$

$$E_i(T) = 0,\ \forall\ i,$$

$$0 \le Y_i(k\Delta t) \le L_i(k\Delta t), \forall\ i,k$$

$$E_i(0) \ge 0,\ \forall\ i,\ \text{and}$$

$$\sum_{i=1}^{M} E_i(0) = E_0.$$

Unlike P0, the decision space in P0D is finite. That is, the decision variables in P0D form a finite set. A solution to P0D optimizes each discharging profile at $N$ uniformly-spaced sampling points, namely $Y_i(\Delta t), \dots, Y_i(N\Delta t)$, and, determines the best energy allocation policy, i.e., $E_1(0), \dots, E_M(0)$, for the assumed discrete-time cost function $\widetilde{\mathsf{EC}}$. With this formulation, a precision-adjustable solution to P0 can be obtained. The higher the sampling frequency, the higher the precision.

*3.3.2. Linearization of $f_i(x)$*

The non-linear relationship between $X_i(t)$ and $Y_i(t)$, which is stated in (3), and later denoted by $f_i(\cdot)$, can be approximated by a piece-wise linear function. Specifically, $f_i(\cdot)$ can be replaced with an approximation $\widetilde{f}_i : \mathbb{R} \to \mathbb{R}$, which will be chosen to minimize linearization errors. To properly choose $\widetilde{f}_i(\cdot)$, note the following properties of $f_i(\cdot)$:

- $f_i : \mathbb{R} \to \mathbb{R}$ is a non-decreasing function, that is, for $x_2 > x_1$, it follows that $f_i(x_2) \ge f_i(x_1)$. This property is proven in Appendix A.
- $f_i : \mathbb{R} \to \mathbb{R}$ is a concave function. That is, the line segment connecting any two points in the curve defined by coordinates $(x, f_i(x))$ lies below that same curve. This property is proven in Appendix A.

Given the concavity of $f_i(\cdot)$, its linear approximation $\widetilde{f}_i(\cdot)$ should be chosen as the point-wise minimum of a set of affine functions:

$$\widetilde{f}_i\,[x] = \min_{j\in\{1,\dots,Q\}} \zeta_{i,j}x + \omega_{i,j}, \tag{9}$$

where $Q \in \mathbb{N}$, and $\zeta_{i,j},\ \omega_{i,j} \in \mathbb{R}$. The more linear segments are used, the more accurate is the approximation in the region $[\Psi_i, \infty)$. As seen, using $\widetilde{f}_i(\cdot)$ does not introduce errors in $[0, \Psi_i]$, as this is the linear region of operation.

Parameters $\zeta_{i,j},\ \omega_{i,j},\ j \in \{1,\dots,Q\}$ can be chosen to minimize the approximation error over the interval $[\Psi_i, Y_{\max}]$, with $Y_{\max} > \Psi_i$. The approximation error can be set as the mean-squared error, i.e.,

$$\epsilon_i = \int_{\Psi_i}^{Y_{\max}} \left[ \widetilde{f}_i(x) - \min\left\{ x, \Psi_i \left[ \frac{x}{\Psi_i} \right]^{\frac{1}{\alpha_i}} \right\} \right]^2 dx. \tag{10}$$

Then, for a given number of linear segments $Q$, the following optimization problem can be solved numerically to determine $\zeta_{i,j}$ and $\omega_{i,j},\ \forall\ i,\ j\ \in\ \{1,\dots,Q\}$:

$$\text{PA:} \quad \min_{\zeta_{i,j},\ \omega_{i,j}} \quad \epsilon_i$$

$$\text{s.t.} \qquad (9).$$

In Appendix B, a heuristic approach to solve PA is presented. The proposed solution will be used to determine $\zeta_{i,j}$ and $\omega_{i,j}$ in closed form, thus reducing the computational time of numerical approaches. The approximation error can be made arbitrarily small by increasing the number of linear segments $(Q)$.

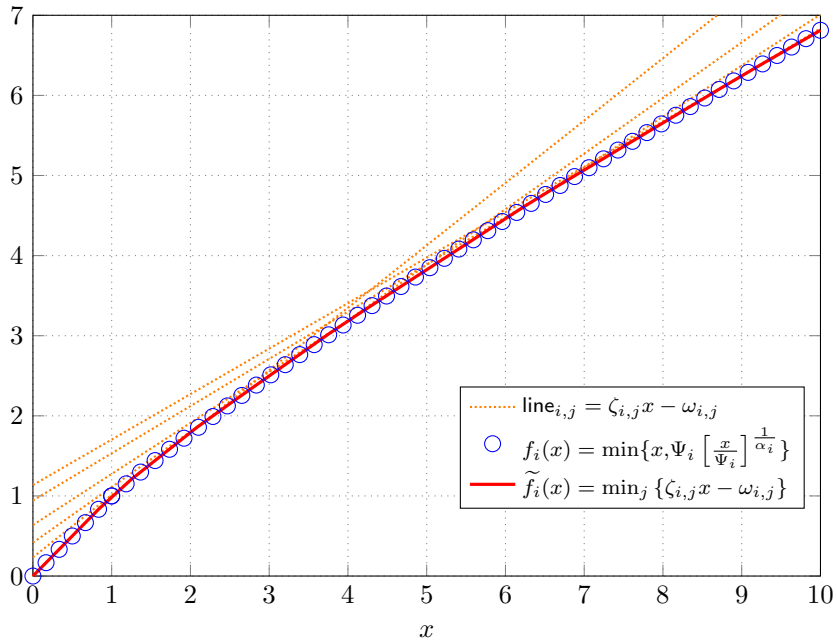


Figure 2: Piece-wise linear approximation of Eq. (3), with $\Psi_i = 1$, $\alpha_i = 1.2$, $\forall\ i$, $Q = 6$. The dotted lines represent tangents to function $f_i(x)$, the solid line is the point-wise minimum across $Q = 6$ lines. The original model is plotted with circular marks.

### 3.3.3. Matrix Formulation

Once discretization and linearization are introduced, the following relaxation can be used to cast P0 as a linear program:

$$Y_i(t) \leq \widetilde{f}_i\left[X_i(t)\right]. \tag{11}$$

This relaxation is introduced to fit the formulation into a linear programming framework. Note that a necessary condition for optimality is to satisfy (11) with equality. Hence, relaxing the original relationship between $Y_i(t)$ and $X_i(t)$ as shown in Eq. (11) will not change the solution to problem P0D.

Constraints $0 \leq E_i(k\Delta t),\ \forall\ k$ can be written in matrix form. That is, for each $i$, it follows that:

$$\Delta t \begin{pmatrix} 1 & 0 & 0 & 0 & \dots & 0 \\ 1 & 1 & 0 & 0 & \dots & 0 \\ 1 & 1 & 1 & 0 & \dots & 0 \\ 1 & 1 & 1 & 1 & \dots & 0 \\ \vdots & \vdots & \vdots & \vdots & \ddots & \vdots \\ 1 & 1 & 1 & 1 & \dots & 1 \end{pmatrix} \begin{pmatrix} X_i(\Delta t) \\ X_i(2\Delta t) \\ X_i(3\Delta t) \\ X_i(4\Delta t) \\ \vdots \\ X_i(N\Delta t) \end{pmatrix} \preceq E_i(0) \begin{pmatrix} 1 \\ 1 \\ 1 \\ 1 \\ \vdots \\ 1 \end{pmatrix}.$$

Note that constraint $E_i(k\Delta t) \leq \Theta_i,\ \forall\ k$ can be ignored because $E_i(t)$ is decreasing in $[0, T]$, as there is no battery charging operations once the energy allocation is completed.

With the considerations explained above, P0D can be cast as a linear program. The accuracy of the solution will depend on the sampling interval $\Delta t$ and the number of linear segments $Q$ used to approximate (3). Therefore, finding a precise solution will require a high computational capacity, which motivates an alternative approach to the problem.

## 4. Proposed Solution

In this section, a method to solve P0 by using calculus of variations is presented. The proposed method leads to a closed-form solution that can be applied in practical scenarios, e.g., when the energy generation capacity is insufficient to meet the load.

To obtain an analytical solution, P0 is divided into two subproblems: First, the optimal discharging operation is designed for each household. Then the energy allocation policy across all participants is optimized. This strategy is known as a master-slave decomposition, Bertsekas (1999), Boyd et al. (2008), and is pertinent to this particular setting because the two subproblems can be coupled through variables $E_1(0), \dots, E_M(0)$.

Specifically, the two subproblems can be cast in terms of $E_1(0), \dots, E_M(0)$ as follows: 1) Given $E_i(0)$, determine the discharging profile $Y_i(t)$, which minimizes the energy cost incurred by the $i$th

household alone. 2) Given that $Y_i(t)$ has been optimized for any arbitrary $E_i(0)$, find the $E_i(0)$'s which minimize the energy cost $\mathsf{EC}$ incurred by all the participating households in $[0, T]$.

The first subproblem is formulated to optimize the trajectory $Y_i(t)$; hence, it can be tackled by using variational techniques, Giaquinta et al. (2004). The second subproblem is formulated to optimize the energy allocation policy, i.e., to design $E_1(0), \ldots, E_M(0)$, and hence, it can be tackled by using more conventional approaches such as Karush-Kuhn-Tucker conditions, Boyd and Vandenberghe (2004).

### *4.1. Optimal Discharging Profiles*

In this section, subproblem 1 is formulated and tackled. Specifically, the aim will be to optimize each $Y_i(t)$ in terms of $E_i(0)$.

#### *4.1.1. Formulation*

To optimize $Y_1(t), \ldots, Y_M(t)$, the following optimization problem is formulated:

$$\begin{aligned} \text{P1: } & \min_{Y_i(t)} \quad \int_0^T P_i(t) \left[ L_i(t) - Y_i(t) \right] dt \\ & \text{s.t. } 0 \leq E_i(t) \leq \Theta_i, \ E_i(T) = 0, \text{ and } Y_i(t) \leq L_i(t), \ \forall \ t, \end{aligned}$$

where $E_i(t)$ is linked to $X_i(t)$ through (2), and $X_i(t)$ is related to $Y_i(t)$ through (3). In this first stage, $Y_i(t)$ is optimized in terms of $E_i(0)$. Therefore, P1 is a simplified version of P0, where the variables $E_1(0), \ldots, E_M(0)$ are no longer part of the design space; they are instead treated as inputs. Variables $E_1(0), \ldots, E_M(0)$ are optimized in a second stage by solving a different optimization problem.

#### *4.1.2. Considerations*

As P0, P1 is not a convex optimization problem. Moreover, P1 also has an infinite number of constraints, as stated by inequalities $0 \leq E_i(t) \leq \Theta_i$, and $Y_i(t) \leq L_i(t)$, $\forall \ t$. P1 can be solved numerically by introducing discretization and linearization to handle the relationship between $X_i(t)$ and $Y_i(t)$. However, to obtain a more insightful result, the following consideration is made:

For $\alpha_i \to 1^+$ the relationship between $X_i(t)$ and $Y_i(t)$, stated in (3), can be simplified to:

$$Y_i(t) = \Psi_i \left[ \frac{X_i(t)}{\Psi_i} \right]^{\frac{1}{\alpha_i}}. \tag{12}$$

The simplification incurs an approximation error only when $X_i(t) < \Psi_i$. Moreover, this error approaches 0, as $\alpha_i \to 1^+$. Practical values of $\alpha_i$ are normally in the range $[1.1, 1.3]$, Tran and Khambadkone (2013). The relationship between the original model and its relaxed version are illustrated in Figs. 3 and 3 for different values of $\alpha_i$ and $\Psi_i$.

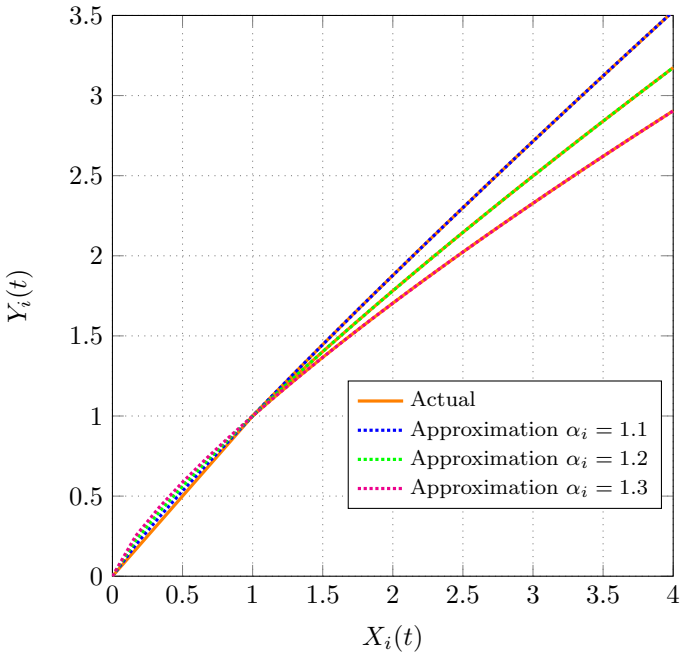


Figure 3: Approximation (12) for different values of $\alpha_i$ with $\Psi_i = 1$. Smaller approximation errors are incurred when $\alpha_i \to 1^+$.

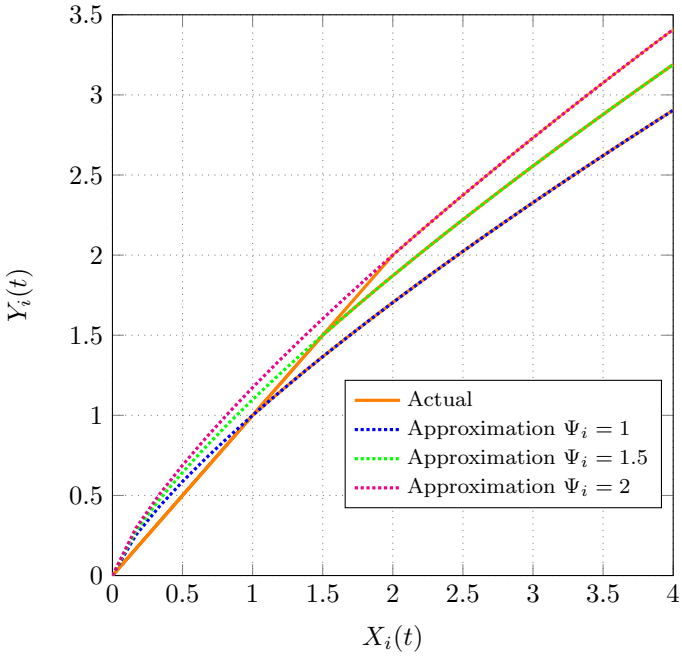


Figure 4: Approximation (12) for different values of $\Psi_i$ with $\alpha_i = 1.3$. Approximation errors are incurred when $X_i(t) < \Psi_i$.

To simplify notation, the optimization problem will be written in terms of $X_i(t)$. Then, with the consideration explained above, P1 simplifies to:

$$\text{P2:} \quad \min_{X_i(t)} \int_0^T P_i(t) \left[ L_i(t) - \Psi_i \left[ \frac{X_i(t)}{\Psi_i} \right]^{\frac{1}{\alpha_i}} \right] dt$$

$$\text{s.t.} \quad \int_0^T X_i(t)dt = E_i(0).$$

In P2, constraint (2) has been replaced with $\int_0^T X_i(t)dt = E_i(0)$. This substitution follows because the $i$th battery is initialized with $E_i(0)$ energy units, as stated in Eq. (2). As the battery state will be non-increasing over time, only constraint $E_i(t) \geq 0$ is considered, and this constraint is satisfied if the total energy discharged over the billing period is at most $E_i(0)$. However, it is clearly suboptimal to use less energy than the one allocated to each household. Therefore, the energy drawn from the battery by the $i$th house in $[0, T]$ has to be exactly $E_i(0)$.

*4.1.3. Solution*

The Euler-Lagrange optimality condition, Giaquinta et al. (2004), can be used to find candidate solutions to P2:

**Lemma 1.** *Subject to* $\int_0^T X_i(t)dt = E_i(0)$, $\alpha_i > 1$, *and* $P_i(t) > 0 \ \forall \ t$, *a necessary condition for* $X_i(t)$ *to minimize the functional*

$$\int_0^T P_i(t) \left[ L_i(t) - \Psi_i \left[ \frac{X_i(t)}{\Psi_i} \right]^{\frac{1}{\alpha_i}} \right] dt$$

*is that* $X_i(t) = X_i^*(t), \ \forall \ t$, *where*

$$X_i^*(t) \triangleq \Psi_i \left[ \frac{P_i(t)}{\lambda} \right]^{\frac{\alpha_i}{\alpha_i - 1}}. \tag{13}$$

*In* (13), $\lambda \in \mathbb{R}$ *is a constant, which can be chosen to comply with constraint* $\int_0^T X_i(t)dt = E_i(0)$.

*Proof.* The Euler-Lagrange condition applied to P2 states that the optimal $X_i(t)$ must satisfy the following differential equation:

$$P_i(t) \frac{\partial}{\partial X_i} \left[ \Psi_i \left[ \frac{X_i(t)}{\Psi_i} \right]^{\frac{1}{\alpha_i}} - \lambda X_i(t) \right] = 0, \tag{14}$$

where $\lambda \in \mathbb{R}$ is the Lagrange multiplier. Eq. (14) yields the following family of candidate solutions: $X_i^*(t) = \Psi_i \left[ \frac{P_i(t)}{\lambda} \right]^{\frac{\alpha_i}{\alpha_i - 1}}$. ■

As seen from Lemma 1, the solution to P2 can be written in terms of $E_i(0)$ through $\lambda$:

$$\lambda = \left[ \frac{E_i(0)}{\Psi_i \int_0^T [P_i(t)]^{\frac{\alpha_i}{\alpha_i - 1}} dt} \right]^{\frac{1 - \alpha_i}{\alpha_i}}, \tag{15}$$

which is obtained after replacing the candidate solution $X_i^*(t)$ in constraint $\int_0^T X_i(t)dt = E_i(0)$.

To simplify notation, let $\gamma_i \triangleq \int_0^T P_i(t)L_i(t)dt$. Then, the optimized energy cost $\mathsf{EC}^*$ can be written in terms of the $E_i(0)$'s by replacing $X_i^*(t)$ in P2's objective, and then, from (1) it follows that:

$$\mathsf{EC}^* = \sum_{i=1}^{M} \left\{ \gamma_i - \left[ \Psi_i \int_0^T [P_i(t)]^{\frac{\alpha_i}{\alpha_i - 1}} \, dt \right]^{\frac{\alpha_i - 1}{\alpha_i}} E_i(0)^{\frac{1}{\alpha_i}} \right\}.$$

*4.2. Optimal Energy Allocation Policy*

In this section, $\mathsf{EC}^*$ is optimized with respect to the $E_i(0)$'s, which must satisfy $\sum_{i=1}^{M} E_i(0) = E_0$ and $E_i(0) \leq \Theta_i \ \forall \ i$. Formally, the following optimization problem is formulated:

$$\begin{aligned} \text{P3:} \quad & \min_{E_1(0),\ldots,E_M(0)} \quad \mathsf{EC}^* \\ & \text{s.t. } 0 \leq E_i(0) \leq \Theta_i \ \forall \ i, \text{ and } \sum_{i=1}^{M} E_i(0) = E_0. \end{aligned}$$

P3 is feasible only if the ESSs across households are such that they have sufficient capacity to store $E_0$ energy units at $t = 0$. Moreover, P3 is a convex optimization problem, as shown in the following lemma:

**Lemma 2.** *If $\alpha_i > 1$, $\Psi_i > 0$, and $P_i(t) \geq 0 \ \forall \ t$, then P3 is a convex optimization problem.*

*Proof.* The objective in P3 is the sum of functions which are convex in $E_1(0), \ldots, E_M(0)$ when $\alpha_i > 1$, $\Psi_i > 0$, and $P_i(t) \geq 0 \ \forall \ t$. To see this, note that $h\left(E_i(0)\right) \triangleq E_i(0)^{\frac{1}{\alpha_i}}$ is concave in $E_i(0)$ for $\alpha_i > 1$, hence

$$\left[ \Psi_i \int_0^T [P_i(t)]^{\frac{\alpha_i}{\alpha_i - 1}} \, dt \right]^{\frac{\alpha_i - 1}{\alpha_i}}$$

should be non-negative, which happens when $\Psi_i > 0$, and $P_i(t) \geq 0 \ \forall \ t$. ■

As stated in Lemma 2, P3 is convex if $\alpha_i > 1$, $\Psi_i > 0$, and $P_i(t) \geq 0 \ \forall \ t$. These requirements imply non-negative prices, non-negative nominal output power, and a Peukert's exponent larger than 1. All of these conditions are accounted for in this model and correspond to practical scenarios.

P3 is solved by using Karush-Kuhn-Tucker conditions, Boyd and Vandenberghe (2004), which will ensure that both equality and inequality constraints are satisfied. The following lemma discusses one of its implications.

**Lemma 3.** *If $\Psi_i > 0$, $\Theta_i \geq E_0$, $\alpha_i = \alpha > 1$, and $P_i(t) \geq 0 \ \forall \ t, \ \forall \ i$, then $\mathsf{EC}^*$ attains its minimum when:*

$$E_i(0) = E_i^*(0) \triangleq \frac{\left(\frac{1}{\eta_i}\right)^{\frac{\alpha}{1-\alpha}}}{\sum_{j=1}^{M} \left(\frac{1}{\eta_j}\right)^{\frac{\alpha}{1-\alpha}}} E_0, \ \forall \ i, \tag{16}$$

*where $\eta_i = \left[ \Psi_i \int_0^T [P_i(t)]^{\frac{\alpha_i}{\alpha_i - 1}} \, dt \right]^{\frac{\alpha_i - 1}{\alpha_i}}$.*

*Proof.* First, the Lagrangian is written as follows:

$$\mathcal{L}\left[E_1(0),\ldots,E_M(0)\right] = \sum_{i=1}^{M}\left[\gamma_i - \eta_i E_i(0)^{\frac{1}{\alpha_i}}\right] + \lambda\left[\sum_{i=1}^{M} E_i(0) - E_0\right] + \sum_{j=1}^{M}\mu_j\left[E_j(0) - \Theta_j\right], \quad (17)$$

where $\lambda$ and $\mu_i,\ i \in \{1,\ldots,M\}$ are Lagrange multipliers. Then, note:

$$\frac{\partial}{\partial E_i(0)}\mathcal{L}\left[E_1(0),\ldots,E_M(0)\right] = -\eta_i\frac{1}{\alpha_i}E_i(0)^{\frac{1-\alpha_i}{\alpha_i}} + \lambda + \mu_i.$$

Hence, the optimality condition $\frac{\partial}{\partial E_i(0)}\mathcal{L} = 0$ yields $E_i(0) = \left[\alpha_i\frac{(\lambda+\mu_i)}{\eta_i}\right]^{\frac{\alpha_i}{1-\alpha_i}},\ \forall\ i$, which substituted in $\sum_{i=1}^{M} E_i(0) = E_0$ leads to

$$\sum_{i=1}^{M}\left[\alpha_i\frac{\lambda+\mu_i}{\eta_i}\right]^{\frac{\alpha_i}{1-\alpha_i}} = E_0. \quad (18)$$

Eq. (18) can be solved numerically through complementary slackness, Boyd and Vandenberghe (2004). That is, whenever $E_i(0) < \Theta_i$ it must be that $\mu_i = 0$, and whenever $\mu_i > 0$, it must follow that $E_i(0) = \Theta_i$. A closed-form solution can be found when $\Theta_i \geq E_0$ and $\alpha_i = \alpha\ \forall\ i$. Specifically, in such a condition, $\lambda$ can be written in terms of $E_0$ as

$$\lambda = \frac{1}{\alpha}\left[\frac{E_0}{\sum_{i=1}^{M}\left[\frac{1}{\eta_i}\right]^{\frac{\alpha}{1-\alpha}}}\right]^{\frac{1-\alpha}{\alpha}},$$

and use this result to obtain (16). ■

As stated in Lemma 3 the optimal energy allocation policy is one in which the optimal $E_i(0)$, denoted by $E_i^*(0)$, is directly proportional to the ratio

$$\delta_i \triangleq \frac{\left(\frac{1}{\eta_i}\right)^{\frac{\alpha}{1-\alpha}}}{\sum_{j=1}^{M}\left(\frac{1}{\eta_j}\right)^{\frac{\alpha}{1-\alpha}}} = \frac{(\eta_i)^{\frac{\alpha}{\alpha-1}}}{\sum_{j=1}^{M}(\eta_j)^{\frac{\alpha}{\alpha-1}}}.$$

Hence, the household with the highest prices and whose battery has the largest nominal output power will take the largest share of $E_0$. If the energy prices were the same across households, and $\alpha_i = \alpha\ \forall\ i$, then the allocation criterion would be determined entirely by the nominal output power of each battery, i.e., by the value of $\Psi_i$.

### *4.3. Estimated Energy Expenses*

In the following, an expression to estimate the cost savings achieved with the proposed strategy is derived. The obtained solutions (13) and (16) are replaced in the cost function to derive the following estimate:

$$\widetilde{\mathsf{EC}}^* = \sum_{i=1}^{M}\gamma_i - [E_0]^{\frac{1}{\alpha}}\left[\sum_{i=1}^{M}\left[\frac{1}{\eta_i}\right]^{\frac{\alpha}{1-\alpha}}\right]^{\frac{\alpha-1}{\alpha}}, \quad (19)$$

where the algebraic steps have been omitted for brevity.

Table 1: Simulation Scenarios

| **Parameter** | **Value** |
|---|---|
| $\{T,\ \Delta t,\ M,\ \Psi,\ Q\}$ | $\{1,\ 0.01,\ 2,\ 1,\ 21\}$ |
| $P_1(t)$ | $\sim \mathcal{U}(0,1)$ |
| $P_2(t)$ | $\sim \mathcal{U}(0,1)$ |
| $L_i(t)$ | $\sim \mathcal{U}(0,1),\ \forall\ i \in \{1,\ldots,M\}$ |

## 5. Numerical Results

In this section, numerical results are provided to validate the analysis presented throughout the paper. This section is divided into five parts. In the first part, the analytical results are verified in simulation. In the second part, the proposed solution is assessed in terms of battery parameters such as the rated output power and Peukert's exponent. In the third part, the optimality of the proposed energy allocation policy is discussed, and results are compared against those obtained with alternative policies. In the fourth part, the significance of the non-linear discharging model is discussed. Specifically, the results obtained with the proposed strategy are compared with those achieved with solutions based on linear ESS models. The fifth part illustrates the optimized discharging schedules obtained with the numerical approach and the proposed calculus-based solution.

Unless otherwise stated, the simulation parameters considered throughout the section follow the definitions in Table 1. To facilitate comparisons, in this section, it is assumed that all the batteries in the community have the same Peukert's exponent and rated output power, respectively denoted by $\alpha$ and $\Psi$, i.e., $\alpha_i = \alpha$ and $\Psi_i = \Psi,\ \forall\ i$. A standard uniform distribution has been assumed to draw pricing signals, as it features the highest entropy among bounded random variables. Moreover, standardized fees allow for a clearer visualization of the results.

The quantities involved in the simulations are specified by using generic measurement units such as time, power, energy, and monetary units, respectively denoted by [TU], [PU], [EU], and [MU]. The average performance of the proposed strategies is determined by considering ten thousand realizations of energy pricing signals drawn from a standard uniform distribution. Finally, throughout this section, the relationship (12) is assumed to comply with $\alpha_i = \alpha > 1,\ \forall\ i$. The number of linear segments used in its piece-wise linear approximation is 21, i.e., $Q = 21$. They are tangent to the curve $f_i(x) = \Psi_i \left[\frac{x}{\Psi_i}\right]^{\frac{1}{\alpha_i}}$ at points $x \in \{0.5\Psi, 1\Psi, 1.5\Psi, 2\Psi, 3\Psi, 4\Psi, 5\Psi, 6\Psi, 7\Psi, 8\Psi, 9\Psi, 10\Psi, 13\Psi, 16\Psi, 20\Psi, 25\Psi, 30\Psi, 40\Psi, 50\Psi, 80\Psi, 100\Psi\}$.

### *5.1. Numerical vs. Analytical Solution*

The average cost savings obtained with the proposed strategy and the discretization-based approach are plotted in Fig. 5. The simulation scenario is summarized in Table 1. The cost savings are defined as the difference between the energy cost incurred when $E_0 = 0$, and the energy cost optimized through

energy allocation, and denoted by $\mathsf{EC}^*$. Formally, the cost savings $\mathsf{CS}$ are defined as

$$\mathsf{CS} = \sum_{i=1}^{M} \left\{ \left[ \Psi_i \int_0^T [P_i(t)]^{\frac{\alpha_i}{\alpha_i - 1}} \, dt \right]^{\frac{\alpha_i - 1}{\alpha_i}} E_i(0)^{\frac{1}{\alpha_i}} \right\}, \tag{20}$$

which intuitively represent the benefit brought in by the energy generated in the farm. As seen in (20), and verified in Fig. 5, the cost savings are concave in $E_i(0)$. This means that higher cost savings are expected with the increase in the generation capacity at the energy farm. Due to losses incurred in the discharging operation, the relationship between the cost savings and $E_i(0)$ is sublinear. As seen in Fig. 5, the two approaches (numerical and analytical) achieve very similar performance across different values of $E_0$. These results then confirm the validity of the analysis developed in Sec. 4.

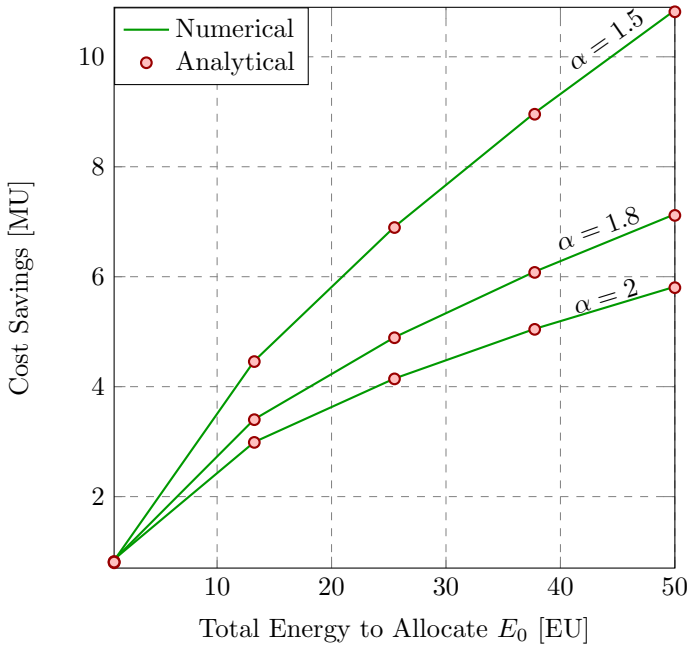


Figure 5: Comparative performance: Numerical vs. analytical solution. The results obtained with the numerical approach match the analytical results.

### *5.2. Impact of Battery Parameters on Performance*

Figs. 6 and 7 show the average cost savings obtained with the proposed strategy for different values of $\alpha$ and $\Psi$, as per the simulation scenario summarized in Table 1. As seen in Fig. 6, smaller $\alpha$ values result in higher cost savings. This result follows from the assumed battery model. Specifically, when $X_i(t) > \Psi$, the power loss incurred in the discharging operation is $\Psi_i \left[\frac{X_i(t)}{\Psi_i}\right]^{\frac{1}{\alpha_i}} - X_i(t)$. Consequently, as $\alpha$ grows, the losses incurred in the discharging operation increase. On the contrary, larger values of $\Psi$ (i.e., $\Psi_i$) lead to smaller power loss and better performance. This is also shown in Fig. 7, where different values of $\Psi$ have been considered.

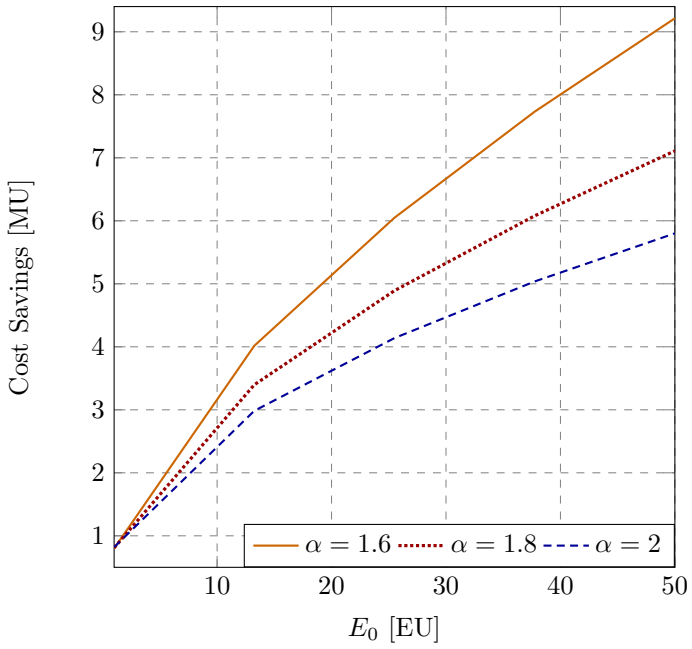


Figure 6: Impact of battery parameters on performance with $\Psi = 1$. The closer is $\alpha$ to $1^+$, the higher are the cost savings. The concavity of the curve follows from the losses incurred in the discharging operation.

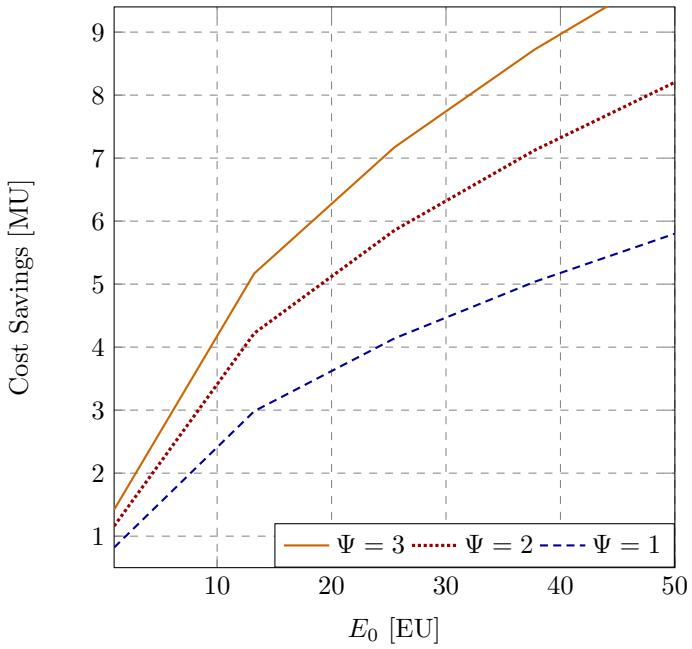


Figure 7: Impact of battery parameters on performance with $\alpha = 2$. The larger is $\Psi$, the higher are the cost savings.

### 5.3. Optimality of Proposed Energy Allocation Policy

Fig. 8 shows the average cost savings obtained with the proposed strategy for different values of $E_1(0)$ while enforcing $E_1(0) + E_2(0) = 10$, and other simulation parameters as per the scenario summarized in Table 1. As seen in Fig. 8, the highest performance is obtained when the energy allocation strategy follows Lemma 3. Again, it is seen that smaller values of $\alpha$ lead to better performance. Moreover, within the scenarios considered, optimizing the energy allocation policy is more critical when $\Psi = 3$ and $\alpha = 2$. This follows because the concavity of $\mathsf{CS}$ grows with $\alpha$.

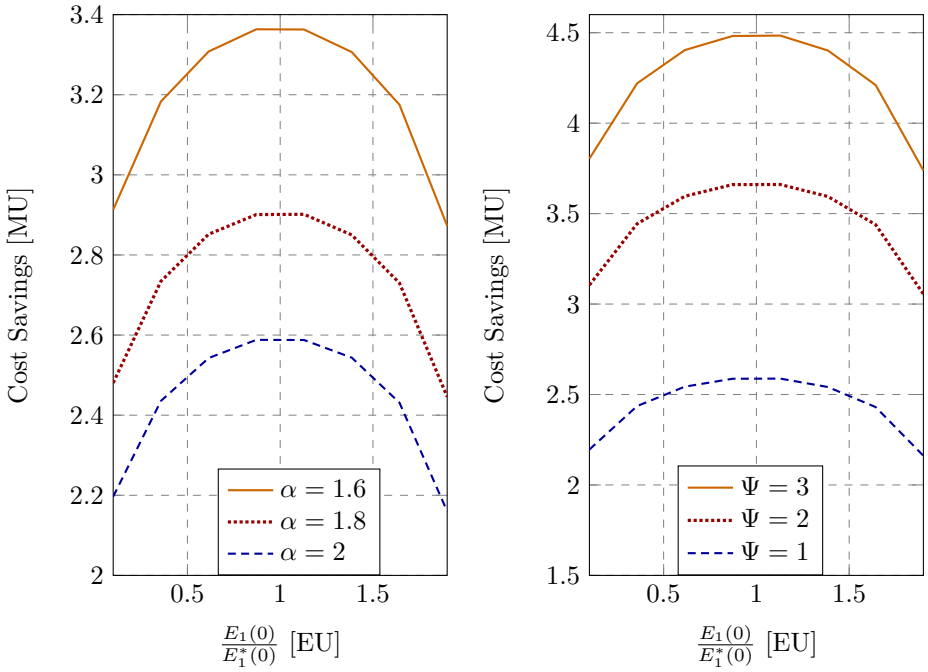


Figure 8: Optimality of the proposed energy allocation policy. Larger $\Psi$ and smaller $\alpha$ lead to better performance.

### 5.4. Comparison with Existing Approaches

This section compares the proposed strategy with existing approaches in the literature, which are based on linear ESS models. The simulation parameters listed in Table 1 are considered. In particular, random pricing signals are assumed, and the results obtained are shown in Fig. 9. As observed, the proposed strategy outperforms solutions based on liner battery models, in particular as $\alpha_i$ increases. This happens because when $\alpha_i$ is large, discharging losses are more significant, and ignoring them leads to a more prominent performance degradation.

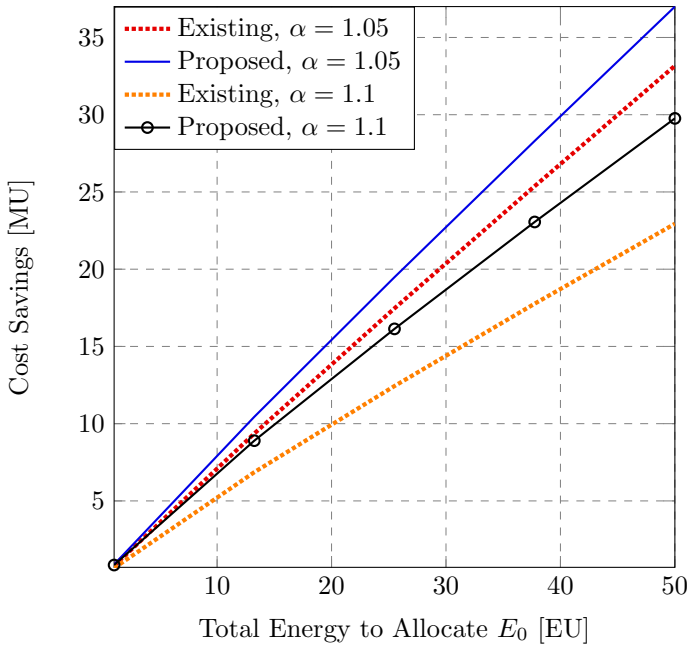


Figure 9: Comparison with approaches based on liner battery models. As seen, disregarding the non-linear characteristics of the ESS results in performance loss. Non-linearity of the battery discharging operation increases with $\alpha$.

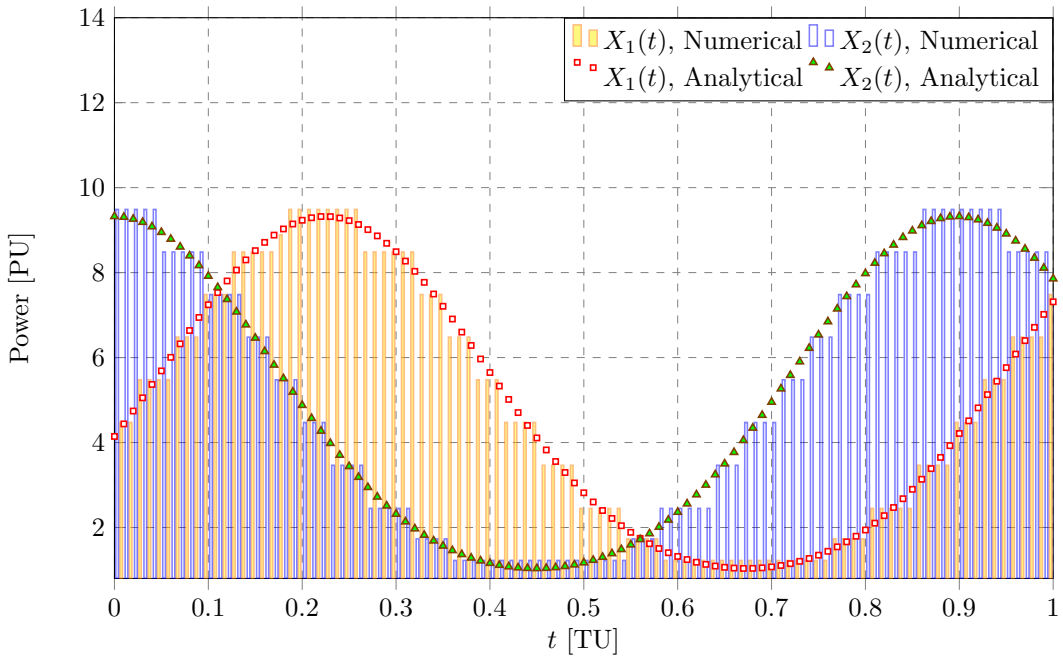


Figure 10: Discharging schedules obtained numerically and analytically with $E_0 = 10$[EU]. Mismatch depends on discretization step size $\Delta t$ and number of linear segments $Q$, used to approximate Eq. (3). In this scenario $\Delta t = 0.01$ and $Q = 21$.

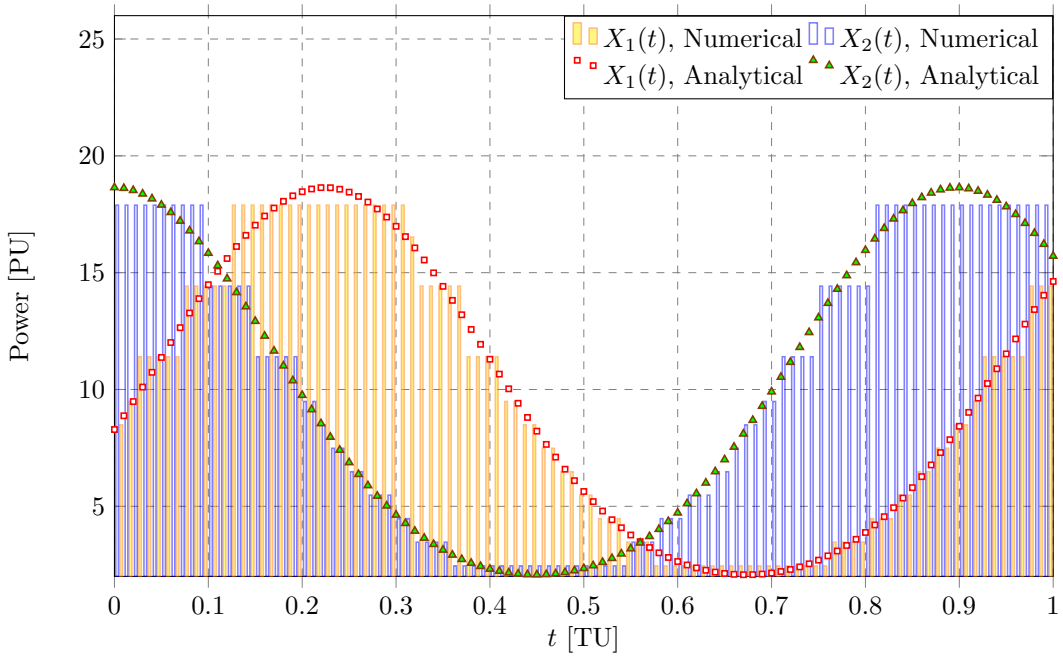


Figure 11: Discharging schedules obtained numerically and analytically with $E_0 = 20$[EU]. Mismatch depends on discretization step size $\Delta t$ and number of linear segments $Q$, used to approximate Eq. (3). In this scenario $\Delta t = 0.01$ and $Q = 21$.

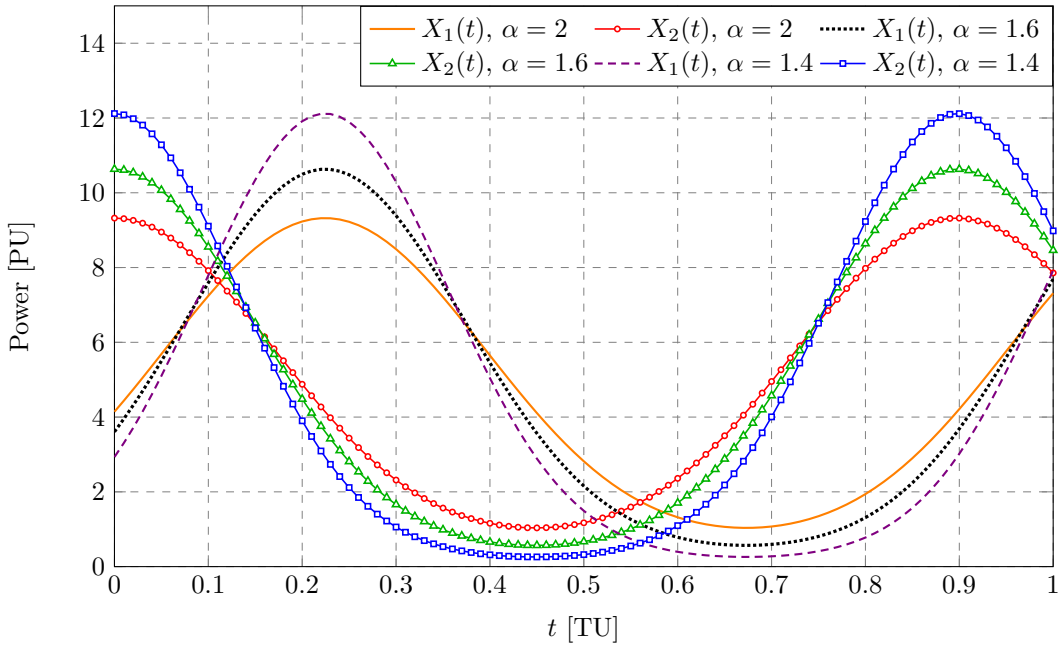


Figure 12: Discharging schedules obtained analytically with $E_0 = 10$[EU]. Price selectivity increases as $\alpha \to 1^+$.

To illustrate the properties of the discharging schedules, the simulation scenario summarized in Table 1 is considered with deterministic pricing signals. Specifically, let $P_1(t) = \sin(7t) + 2$ and $P_2(t) = \cos(7t) + 2$. Then, the discharging profiles obtained with the numerical approach and the proposed strategy are shown in Fig. 10. As seen, the two solutions agree up to some gap, which depends on the accuracy of the numerical approach. The accuracy of the solution obtained through discretization and linearization depends on the discretization step and the number of linear segments used to approximate (3). It is also observed that the numerical approach is more accurate when the optimized value of $X_i(t)$ is below 10 [PU]. This follows because the number of linear segments used to approximate (3) is larger for $X_i(t) < 10\Psi_i$. Finally, as expected, the discharging schedules track the pricing signals valid for each household. Moreover, price selectivity increases when $\alpha$ approaches $1^+$, as shown in Fig. 12.

## 6. Conclusions

This paper presents a framework to optimize energy utilization through battery management in a cooperative environment. In the setting assumed, households share access to a community-owned energy farm. The proposed framework considers the non-linear characteristics of the discharging operation and can be used to minimize the energy expenditure incurred by participating households over a finite planning horizon. Location- and time-dependent electricity prices are considered for generality.

A relaxed version of the optimization problem is solved in closed form by using calculus of variations. The solution consists of optimal discharging schedules and an energy allocation policy. Using these results, several mathematical expressions are derived to estimate the cost savings achieved with the proposed strategy over a finite planning horizon.

Simulations demonstrate how the proposed strategy outperforms existing solutions based on linear battery models. Moreover, the analytical results are verified through numerical computations. The proposed strategy is also evaluated in terms of battery parameters such as efficiency rate and rated output power.

The numerical results presented in this paper clearly demonstrate that discharging schedules can be affected by time-dependent energy prices and battery efficiency rates. Specifically, to maximize cost savings, discharging schedules need to track price signals. Moreover, price-selectivity increases with higher battery efficiency rates. That is, low efficiency rates in battery operations hinder price-responsiveness.

In cooperative environments, proper energy allocation has been shown to increase saving potential. Energy allocation policies should be devised to maximize the common good, particularly, in situations where pricing signals are location-dependent or when the participating storage units differ across

characteristics such as size and efficiency.

The analytical results obtained in this paper can be used to reduce the computational complexity of energy optimization strategies involving storage management. The performance estimates derived can be used to assess the potential of cooperative energy optimization in communities with shared energy generation facilities.

## 7. Nomenclature

| | |
|---|---|
| $L_i(\cdot)$ | Power consumed by the $i$th household |
| $P_i(\cdot)$ | Time-varying energy prices, $i$th household |
| $X_i(\cdot)$ | Power drawn from the storage, $i$th household |
| $Y_i(\cdot)$ | Effective power drawn from storage, $i$th household |
| $E_i(\cdot)$ | Energy stored in the battery of the $i$th house over time |
| $\alpha_i$ | Peukert's exponent, battery of the $i$th house |
| $\Psi_i$ | Rated power output, battery of the $i$th house |
| $\Theta_i$ | Storage capacity, battery of the $i$th house |
| $\preceq$ | Element-wise $\leq$ |
| $X \sim \mathcal{U}(a,b)$ | $X$ is uniformly distributed in $[a,b]$ |

## Appendix A: Properties of $f_i(x)$

*Non-Decreasing Function*

For $\alpha_i > 1$ and $\Psi_i > 0$ the function $f_i(x)$, defined as $f_i(x) \triangleq \min\left\{x, \Psi_i\left[\frac{x}{\Psi_i}\right]^{\frac{1}{\alpha_i}}\right\}$, is non-decreasing.

*Proof.* If $f_i(x)$ is non-decreasing, for $x_2 > x_1$, it must follow that $\min\left\{x_2, \Psi_i\left[\frac{x_2}{\Psi_i}\right]^{\frac{1}{\alpha_i}}\right\} > \min\left\{x_1, \Psi_i\left[\frac{x_1}{\Psi_i}\right]^{\frac{1}{\alpha_i}}\right\}$. To see this, consider the following cases:

1. $x_1 < \Psi_i$ and $x_2 < \Psi_i$. In this case, $\min\left\{x_1, \Psi_i\left[\frac{x_1}{\Psi_i}\right]^{\frac{1}{\alpha_i}}\right\} = x_1$ and $\min\left\{x_2, \Psi_i\left[\frac{x_2}{\Psi_i}\right]^{\frac{1}{\alpha_i}}\right\} = x_2$, and hence the property holds for any $x_2 > x_1$.
2. $x_1 < \Psi_i$ and $x_2 > \Psi_i$. In this case, $\min\left\{x_1, \Psi_i\left[\frac{x_1}{\Psi_i}\right]^{\frac{1}{\alpha_i}}\right\} = x_1$ and $\min\left\{x_2, \Psi_i\left[\frac{x_2}{\Psi_i}\right]^{\frac{1}{\alpha_i}}\right\} = \Psi_i\left[\frac{x_2}{\Psi_i}\right]^{\frac{1}{\alpha_i}}$. Since $x_2 > \Psi_i$, for $\Psi_i > 0$ and $\alpha_i > 1$, it follows that
$$x_2 > \Psi_i\left[\frac{x_2}{\Psi_i}\right]^{\frac{1}{\alpha_i}} > \Psi_i > x_1.$$
Therefore, for $x_2 > x_1$, $\min\left\{x_2, \Psi_i\left[\frac{x_2}{\Psi_i}\right]^{\frac{1}{\alpha_i}}\right\} > \min\left\{x_1, \Psi_i\left[\frac{x_1}{\Psi_i}\right]^{\frac{1}{\alpha_i}}\right\}$, also in this case.
3. $x_1 > \Psi_i$ and $x_2 < \Psi_i$. This case is infeasible because initially it was considered that $x_2 > x_1$.

4. $x_1 > \Psi_i$ and $x_2 > \Psi_i$. In this case, $\min\left\{x_1, \Psi_i\left[\frac{x_1}{\Psi_i}\right]^{\frac{1}{\alpha_i}}\right\} = \Psi_i\left[\frac{x_1}{\Psi_i}\right]^{\frac{1}{\alpha_i}}$ and $\min\left\{x_2, \Psi_i\left[\frac{x_2}{\Psi_i}\right]^{\frac{1}{\alpha_i}}\right\} = \Psi_i\left[\frac{x_2}{\Psi_i}\right]^{\frac{1}{\alpha_i}}$. Clearly, if $x_2 > x_1$, then $\Psi_i\left[\frac{x_2}{\Psi_i}\right]^{\frac{1}{\alpha_i}} > \Psi_i\left[\frac{x_1}{\Psi_i}\right]^{\frac{1}{\alpha_i}}$.

■

*Concave Function*

*Proof.* Given that $f_i(x)$ is non differentiable over its entire domain, the definition of concavity will be used to prove this property. To prove that $f_i(x)$ is concave, it suffices to show that for any $\theta \in [0,1]$ the following inequality holds:

$$\theta f_i(x) + (1-\theta) f_i(y) \leq f_i\left(\theta x + (1-\theta) y\right), \tag{21}$$

for any $x, y \in \mathbf{dom}\ f_i$. Replacing the definition of $f_i(x)$ in (21) yields:

$$\theta \min\left\{x, \Psi_i\left[\frac{x}{\Psi_i}\right]^{\frac{1}{\alpha_i}}\right\} + (1-\theta)\min\left\{y, \Psi_i\left[\frac{y}{\Psi_i}\right]^{\frac{1}{\alpha_i}}\right\} \leq \min\left\{\theta x + (1-\theta)y, \Psi_i\left[\frac{\theta x + (1-\theta)y}{\Psi_i}\right]^{\frac{1}{\alpha_i}}\right\}. \tag{22}$$

Note that when $\theta = 0$ or $\theta = 1$, the inequality (22) holds for any $x \in \mathbb{R}$ or $y \in \mathbb{R}$. Hence, to prove (22) consider $\theta \in (0,1)$ in each of the following cases:

1. $x < \Psi_i$ and $y < \Psi_i$: In this case, (22) becomes:

$$\theta x + (1-\theta)y \leq \min\left\{\theta x + (1-\theta)y, \Psi_i\left[\frac{\theta x + (1-\theta)y}{\Psi_i}\right]^{\frac{1}{\alpha_i}}\right\}. \tag{23}$$

Since $x < \Psi_i$ and $y < \Psi_i$, for $\theta \in (0,1)$ it follows that $\theta x < \theta\Psi_i$ and $(1-\theta)y < (1-\theta)\Psi_i$. Moreover, if these two inequalities are combined, the result is $\theta x + (1-\theta)y < \Psi_i$. This result implies that

$$\min\left\{\theta x + (1-\theta)y, \Psi_i\left[\frac{\theta x + (1-\theta)y}{\Psi_i}\right]^{\frac{1}{\alpha_i}}\right\} = \theta x + (1-\theta)y,$$

from which it can be seen that (23) follows immediately for $\theta \in (0,1)$.

2. $x < \Psi_i$ and $y > \Psi_i$: In this case, (22) becomes:

$$\theta x + (1-\theta)\Psi_i\left[\frac{y}{\Psi_i}\right]^{\frac{1}{\alpha_i}} \leq \min\left\{\theta x + (1-\theta)y, \Psi_i\left[\frac{\theta x + (1-\theta)y}{\Psi_i}\right]^{\frac{1}{\alpha_i}}\right\}, \tag{24}$$

which will be shown in two steps. First, consider $\theta$ values for which $\theta x + (1-\theta)y \leq \Psi_i$, and hence

$$\min\left\{\theta x + (1-\theta)y, \Psi_i\left[\frac{\theta x + (1-\theta)y}{\Psi_i}\right]^{\frac{1}{\alpha_i}}\right\} = \theta x + (1-\theta)y.$$

As a result, inequality (24) becomes

$$\theta x + (1-\theta)\Psi_i \left[\frac{y}{\Psi_i}\right]^{\frac{1}{\alpha_i}} \leq \theta x + (1-\theta)y,$$

which holds true for $y > \Psi_i > 0$ and $\alpha_1 > 1$. Now examine the case in which $\theta$ is such that $\theta x + (1-\theta)y \geq \Psi_i$. In such a case, inequality (24) becomes

$$\theta x + (1-\theta)\Psi_i \left[\frac{y}{\Psi_i}\right]^{\frac{1}{\alpha_i}} \leq \Psi_i \left[\frac{\theta x + (1-\theta)y}{\Psi_i}\right]^{\frac{1}{\alpha_i}},$$

which also holds true. To see this, note the following development: Without loss of generality, let $x = k_x\Psi_i$ and $y = k_y\Psi_i$ for $k_x \in [0,1)$ and $k_y \in (1,\infty)$, respectively. Replacing these definitions in inequality (24) yields:

$$\theta k_x\Psi_i + (1-\theta)\Psi_i \left[\frac{k_y\Psi_i}{\Psi_i}\right]^{\frac{1}{\alpha_i}} \leq \Psi_i \left[\frac{\theta k_x\Psi_i + (1-\theta)k_y\Psi_i}{\Psi_i}\right]^{\frac{1}{\alpha_i}}$$

which, given $\Psi_i > 0$, can further simplify as follows:

$$\theta k_x + (1-\theta)\left[k_y\right]^{\frac{1}{\alpha_i}} \leq \left[\theta k_x + (1-\theta)k_y\right]^{\frac{1}{\alpha_i}}. \tag{25}$$

Given that $k_x \in [0,1)$, the left-hand side of inequality (25) satisfies:

$$\theta k_x + (1-\theta)\left[k_y\right]^{\frac{1}{\alpha_i}} \leq \theta k_x^{\frac{1}{\alpha_i}} + (1-\theta)\left[k_y\right]^{\frac{1}{\alpha_i}}.$$

Moreover, given the concavity[2] of the function $g_i(x) = x^{\frac{1}{\alpha_i}}$ in $[0,\infty)$:

$$\theta k_x^{\frac{1}{\alpha_i}} + (1-\theta)\left[k_y\right]^{\frac{1}{\alpha_i}} \leq \left[\theta k_x + (1-\theta)k_y\right]^{\frac{1}{\alpha_i}}.$$

After combining the last two inequalities, (25) is obtained.

360 3. $x > \Psi_i$ and $y < \Psi_i$: This case is analogous to case 3, and hence inequality (22) will hold under the same arguments.

4. $x > \Psi_i$ and $y > \Psi_i$: In this case, for $\theta \in (0,1)$, it follows that $\theta x + (1-\theta)y > \Psi_i$, and (22) becomes:

$$\theta\Psi_i \left[\frac{x}{\Psi_i}\right]^{\frac{1}{\alpha_i}} + (1-\theta)\Psi_i \left[\frac{y}{\Psi_i}\right]^{\frac{1}{\alpha_i}} \leq \Psi_i \left[\frac{\theta x + (1-\theta)y}{\Psi_i}\right]^{\frac{1}{\alpha_i}}. \tag{26}$$

Without loss of generality, let $x = k_x\Psi_i$ and $y = k_y\Psi_i$ for $k_x \in [0,1)$ and $k_y \in (1,\infty)$, respectively. Replacing these definitions in inequality (26) yields:

$$\theta\Psi_i \left[\frac{k_x\Psi_i}{\Psi_i}\right]^{\frac{1}{\alpha_i}} + (1-\theta)\Psi_i \left[\frac{k_y\Psi_i}{\Psi_i}\right]^{\frac{1}{\alpha_i}} \leq \Psi_i \left[\frac{\theta k_x\Psi_i + (1-\theta)k_y\Psi_i}{\Psi_i}\right]^{\frac{1}{\alpha_i}}, \tag{27}$$

[2]Function $g_i(x) = x^{\frac{1}{\alpha_i}}$ is concave in $[0,\infty)$ for $\alpha_i > 1$. This can be proven by noting that $\frac{d^2}{dx^2}[g_i(x)] < 0 \; \forall \; x \in [0,\infty)$.

which, for $\Psi_i > 0$ simplifies to:

$$\theta \left[k_x\right]^{\frac{1}{\alpha_i}} + (1-\theta)\left[k_y\right]^{\frac{1}{\alpha_i}} \leq \left[\theta k_x + (1-\theta)k_y\right]^{\frac{1}{\alpha_i}} .$$

This last inequality follows immediately from the concavity of function $g_i(x) = x^{\frac{1}{\alpha_i}}$ in $[0, \infty)$, for $\alpha_i > 1$.

■

## Appendix B: Solving PA

PA can be solved numerically, or by using the following heuristic approach: The line segments $\zeta_{i,j} X_i(t) + \omega_{i,j}$ are chosen as tangent lines to the curve $Y_i(t) = \Psi_i \left[\frac{X_i(t)}{\Psi_i}\right]^{\frac{1}{\alpha_i}}$ at equally-spaced points. Thus, $\zeta_{i,j}$ can be chosen as the slope of the curve, and $\omega_{i,j}$ can be set to ensure that the line $\zeta_{i,j} X_i(t) + \omega_{i,j}$ touches the curve at the specified point. That is, at the $j$th point $X_i(t) = x_j$, $\zeta_{i,j}$ and $\omega_{i,j}$ are given by:

$$\zeta_{i,j} = \frac{1}{\alpha_i}\left[\frac{x_j}{\Psi_i}\right]^{\frac{1-\alpha_i}{\alpha_i}} , \tag{28}$$

and

$$\omega_{i,j} = \Psi_i \left[\frac{x_j}{\Psi_i}\right]^{\frac{1}{\alpha_i}} - \frac{1}{\alpha_i}\left[\frac{x_j}{\Psi_i}\right]^{\frac{1-\alpha_i}{\alpha_i}} x_j. \tag{29}$$

## References


International Energy Agency, Renewables information 2014, Paris, 2014. doi:10.1787/renew-2014-en.

P. Dimitrov, L. Piroddi, M. Prandini, Distributed allocation of a shared energy storage system in a microgrid, in: 2016 American Control Conference (ACC), 2016, pp. 3551–3556. doi:10.1109/ACC.2016.7525464.

D. Feldman, A. M. Brockway, E. Ulrich, R. Margolis, Shared Solar: Current Landscape, Market Potential, and the Impact of Federal Securities Regulation, Technical Report NREL/TP-6A20-63892, 2015.

S. Zhao, X. Lin, M. Chen, Robust online algorithms for peak-minimizing ev charging under multistage uncertainty, IEEE Transactions on Automatic Control 62 (2017) 5739–5754. doi:10.1109/TAC.2017.2699290.

M. R. Sandgani, S. Sirouspour, Coordinated optimal dispatch of energy storage in a network of grid-connected microgrids, IEEE Trans. Sustainable Energy 8 (2017) 1166–1176. doi:10.1109/TSTE.2017.2664666.

N. Gatsis, G. B. Giannakis, Decomposition algorithms for market clearing with large-scale demand response, IEEE Trans. Smart Grid 4 (2013) 1976–1987. doi:10.1109/TSG.2013.2258179.

B. Zhang, R. Rajagopal, D. Tse, Network risk limiting dispatch: Optimal control and price of uncertainty, IEEE Transactions on Automatic Control 59 (2014) 2442–2456. doi:10.1109/TAC.2014.2325640.

K. Rahbar, M. R. V. Moghadam, S. K. Panda, T. Reindl, Shared energy storage management for renewable energy integration in smart grid, in: IEEE Power Energy Society Innovative Smart Grid Technologies Conference (ISGT), 2016, pp. 1–5. doi:10.1109/ISGT.2016.7781230.

Z. Wang, C. Gu, F. Li, P. Bale, H. Sun, Active demand response using shared energy storage for household energy management, IEEE Trans. Smart Grid 4 (2013) 1888–1897. doi:10.1109/TSG.2013.2258046.

M. Rastegar, M. Fotuhi-Firuzabad, H. Zareipour, M. Moeini-Aghtaieh, A probabilistic energy management scheme for renewable-based residential energy hubs, IEEE Transactions on Smart Grid 8 (2017) 2217–2227. doi:10.1109/TSG.2016.2518920.

E. Ratnam, S. Weller, C. Kellett, An optimization-based approach to scheduling residential battery storage with solar PV: Assessing customer benefit, Renewable Energy 75 (2015) 123–134.

V. Pilloni, A. Floris, A. Meloni, L. Atzori, Smart Home Energy Management Including Renewable Sources: A QoE-Driven Approach, IEEE Transactions on Smart Grid 9 (2018) 2006–2018. doi:10.1109/TSG.2016.2605182.

I. Ranaweera, O.-M. Midtgård, Optimization of operational cost for a grid-supporting PV system with battery storage, Renewable Energy 88 (2016) 262–272.

E. Hooshmand, A. Rabiee, Energy management in distribution systems, considering the impact of reconfiguration, RESs, ESSs and DR: A trade-off between cost and reliability, Renewable Energy 139 (2019) 346–358.

W. Tushar, B. Chai, C. Yuen, S. Huang, D. B. Smith, H. V. Poor, Z. Yang, Energy storage sharing in smart grid: A modified auction-based approach, IEEE Trans. Smart Grid 7 (2016) 1462–1475. doi:10.1109/TSG.2015.2512267.

H. K. Nunna, A. M. Saklani, A. Sesetti, S. Battula, S. Doolla, D. Srinivasan, Multi-agent based demand response management system for combined operation of smart microgrids, Sustainable Energy, Grids and Networks 6 (2016) 25 – 34. doi:http://dx.doi.org/10.1016/j.segan.2016.01.002.

T. Cortés-Arcos, J. L. Bernal-Agustín, R. Dufo-López, J. M. Lujano-Rojas, J. Contreras, Multi-objective demand response to real-time prices (RTP) using a task scheduling methodology, Energy 138 (2017) 19 – 31.

I. S. Bayram, M. Abdallah, A. Tajer, K. A. Qaraqe, A stochastic sizing approach for sharing-based energy storage applications, IEEE Trans. Smart Grid 8 (2017) 1075–1084. doi:10.1109/TSG.2015.2466078.

K. Paridari, A. Parisio, H. Sandberg, K. H. Johansson, Demand response for aggregated residential consumers with energy storage sharing, in: 54th IEEE Conf. Decision and Control (CDC), 2015, pp. 2024–2030. doi:10.1109/CDC.2015.7402504.

I. Ranaweera, O.-M. Midtgård, M. Korpås, Distributed control scheme for residential battery energy storage units coupled with PV systems, Renewable Energy 113 (2017) 1099–1110.

N. Liu, X. Yu, W. Fan, C. Hu, T. Rui, Q. Chen, J. Zhang, Online Energy Sharing for Nanogrid Clusters: A Lyapunov Optimization Approach, IEEE Transactions on Smart Grid 9 (2018) 4624–4636. doi:10.1109/TSG.2017.2665634.

D. Tran, A. M. Khambadkone, Energy management for lifetime extension of energy storage system in micro-grid applications, IEEE Trans. Smart Grid 4 (2013) 1289–1296. doi:10.1109/TSG.2013.2272835.

J. Leithon, T. J. Lim, S. Sun, Battery-aided demand response strategy under continuous-time block pricing, IEEE Trans. Signal Process. 64 (2016) 395–405. doi:10.1109/TSP.2015.2483487.

T. AlSkaif, M. G. Zapata, B. Bellalta, A reputation-based centralized energy allocation mechanism for microgrids, in: IEEE Int. Conf. Smart Grid Communications (SmartGridComm), 2015, pp. 416–421. doi:10.1109/SmartGridComm.2015.7436336.

J. Leithon, S. Sun, T. J. Lim, Demand response and renewable energy management using continuous-time optimization, IEEE Transactions on Sustainable Energy 9 (2018) 991–1000. doi:10.1109/TSTE.2017.2771359.

Z. Wang, C. Gu, F. Li, Flexible operation of shared energy storage at households to facilitate PV penetration, Renewable Energy 116 (2018) 438–446.

D. Zhao, H. Wang, J. Huang, X. Lin, Pricing-based energy storage sharing and virtual capacity allocation, in: IEEE Int. Conf. Communications (ICC), 2017, pp. 1–6. doi:10.1109/ICC.2017.7997120.

C. P. Mediwaththe, E. R. Stephens, D. B. Smith, A. Mahanti, A dynamic game for electricity load management in neighborhood area networks, IEEE Trans. Smart Grid 7 (2016) 1329–1336. doi:10.1109/TSG.2015.2438892.

G. Ye, G. Li, D. Wu, X. Chen, Y. Zhou, Towards cost minimization with renewable energy sharing in cooperative residential communities, IEEE Access 5 (2017) 11688–11699. doi:10.1109/ACCESS.2017.2717923.

S. R. Etesami, W. Saad, N. B. Mandayam, H. V. Poor, Stochastic games for the smart grid energy management with prospect prosumers, IEEE Transactions on Automatic Control 63 (2018) 2327–2342. doi:10.1109/TAC.2018.2797217.

Z. Zhang, N. Rahbari-Asr, M. Y. Chow, Asynchronous distributed cooperative energy management through gossip-based incremental cost consensus algorithm, in: 2013 North American Power Symposium (NAPS), 2013, pp. 1–6. doi:10.1109/NAPS.2013.6666854.

I. Stoyanova, M. Biglarbegian, A. Monti, Cooperative energy management approach for short-term compensation of demand and generation variations, in: 2014 IEEE Int. Systems Conf. Proceedings, 2014, pp. 559–566. doi:10.1109/SysCon.2014.6819311.

A. C. Luna, N. L. Diaz, M. Graells, J. C. Vasquez, J. M. Guerrero, Cooperative energy management for a cluster of households prosumers, IEEE Trans. Consumer Electronics 62 (2016) 235–242. doi:10.1109/TCE.2016.7613189.

F. Mangiatordi, E. Pallotti, D. Panzieri, L. Capodiferro, Multi agent system for cooperative energy management in microgrids, in: 2016 IEEE 16th Int. Conf. on Environment and Electrical Engineering (EEEIC), 2016, pp. 1–5. doi:10.1109/EEEIC.2016.7555822.

K. Rahbar, C. C. Chai, R. Zhang, Energy cooperation optimization in microgrids with renewable energy integration, IEEE Trans. Smart Grid PP (2016) 1–1. doi:10.1109/TSG.2016.2600863.

H. Dagdougui, A. Ouammi, L. Dessaint, R. Sacile, Global energy management system for cooperative networked residential green buildings, IET Renewable Power Generation 10 (2016) 1237–1244. doi:10.1049/iet-rpg.2015.0282.

Q. Xu, X. Hu, P. Wang, J. Xiao, P. Tu, C. Wen, M. Y. Lee, A Decentralized Dynamic Power Sharing Strategy for Hybrid Energy Storage System in Autonomous DC Microgrid, IEEE Trans. Industrial Electronics 64 (2017) 5930–5941. doi:10.1109/TIE.2016.2608880.

E. Hammad, A. Farraj, D. Kundur, Grid-independent cooperative microgrid networks with high renewable penetration, in: Proc. IEEE PES Innovative Smart Grid Technologies Conference, Washington DC, 2015, pp. 1–5.

X. Zhou, E. DallAnese, L. Chen, A. Simonetto, An incentive-based online optimization framework for distribution grids, IEEE Transactions on Automatic Control 63 (2018) 2019–2031. doi:10.1109/TAC.2017.2760284.

M. Marzband, F. Azarinejadian, M. Savaghebi, E. Pouresmaeil, J. M. Guerrero, G. Lightbody, Smart transactive energy framework in grid-connected multiple home microgrids under independent and coalition operations, Renewable Energy 126 (2018) 95–106.

Y. Zhang, N. Gatsis, G. B. Giannakis, Robust energy management for microgrids with high-penetration renewables, IEEE Transactions on Sustainable Energy 4 (2013) 944–953. doi:10.1109/TSTE.2013.2255135.

A. Chiş, V. Koivunen, Coalitional game-based cost optimization of energy portfolio in smart grid communities, IEEE Transactions on Smart Grid 10 (2019) 1960–1970. doi:10.1109/TSG.2017.2784902.

J. Leithon, S. Werner, V. Koivunen, Cost-aware renewable energy management: Centralized vs. distributed generation, Renewable Energy 147 (2020) 1164 – 1179. URL: http://www.sciencedirect.com/science/article/pii/S0960148119314089. doi:https://doi.org/10.1016/j.renene.2019.09.077.

M. Giaquinta, S. Hildebrandt, S. O. service), Calculus of Variations I, volume 310., Springer Berlin Heidelberg, Berlin, Heidelberg, 2004.

S. Boyd, L. Vandenberghe, Convex Optimization, Cambridge University Press, New York, NY, USA, 2004.

D. Linden, T. B. Reddy, Handbook of batteries, 3rd ed., McGraw-Hill, New York, 2001.

H. Bao, R. Lu, A New Differentially Private Data Aggregation With Fault Tolerance for Smart Grid Communications, IEEE Internet of Things J. 2 (2015) 248–258. doi:10.1109/JIOT.2015.2412552.

Q. Sun, H. Li, Z. Ma, C. Wang, J. Campillo, Q. Zhang, F. Wallin, J. Guo, A Comprehensive Review of Smart Energy Meters in Intelligent Energy Networks, IEEE Internet of Things J. 3 (2016) 464–479. doi:10.1109/JIOT.2015.2512325.

D. P. Bertsekas, Nonlinear programming, 2nd ed., Athena Scientific, Belmont, Mass, 1999.

S. Boyd, L. Xiao, A. Mutapcic, J. M. y, Notes on decomposition methods, 2008. URL: https://see.stanford.edu/materials/lsocoee364b/08-decomposition_notes.pdf, Notes for EE364B, Stanford University, Winter 2006-07.